INTERFACIAL REACTIONS BETWEEN COAL–AND PETCOKE–SLAGS AND REFRACTORY MATERIALS

Jinichiro Nakano, James Bennett & Kyei-Sing Kwong
National Energy Technology Laboratory (NETL), USA

Sridhar Seetharaman & Tyler Moss
Carnegie Mellon University (CMU), USA

ABSTRACT

The interfacial interactions of coal and petcoke slags with high chromia and alumina refractories were studied by Confocal Scanning Laser Microsopy and Scanning Electron Microscopy with X-ray Energy Dispersive Spectroscopy. The petcoke slag revealed the lower initial deformation temperature as well as lower melting temperature, than the coal slag. The high chromia refractory, in general, performed more effectively in terms of corrosion/erosion resistance against both slags. The alumina substrate, however, surpassed the high chromia refractory in minimizing the slag penetration when the petcoke was placed over a fine grain matrix. The instant formation of the (V, Cr, Fe)O_x layer was noted at the petcoke slag/high chromia interface while discrete particles of (V, Al, Si)O_x were observed at the petcoke slag/alumina interface.

INTRODUCTION

Coal gasifiers are commercially utilized to produce syngas (CO and H_2) from different carbon feedstock, water and oxygen. The syngas is then used to produce chemicals and electric power. Feedstock materials such as coal, petroleum coke (petcoke), natural gas, or biomass contain numerous different minerals which, usually liquefy under the gasification conditions (T = 1300 to 1600°C, P = 2.75 MPa and $\log(P_{O2})$ = -9 to -7 (atm) [7]). This results in the formation of a slag layer on the refractory wall.

One obstacle to achieving greater reliability is the severe slag attack of refractory liners. The slag-refractory interactions occur by a combination of chemical dissolution, mechanical erosion, peeling wear, periodical oxidation-reduction reactions, chemistry variation of feedstock, *etc.* [7]. The mineral impurities impart different chemical and physical properties to the slag, and can interact differently with the refractory liner. Superior corrosion resistance of high chromia containing refractory over alumina has been reported [7, 8, 12]. By cup-type experiments, Rewers *et al.* found that while dissolution of Cr into coal slag was still observed, the spinel $(Al, Cr, Fe)_3O_4$ phase on the refractory side of the coal slag/high chromia refractory interface was still observed [12].

Coal ash slag is comprised mainly of SiO, Al_2O_3, CaO, Fe_2O_3, K_2O and SO_3 plus a balance of TiO_2, P_2O_5, MgO, Na_2O, *etc.*, according to a statistical evaluation over more than 300 samples [15]. Petcoke slag typically contains a large amount of vanadium and consists mainly of SiO_2, Al_2O_3, CaO, Fe_2O_3, K_2O, SO_3, NiO and V_2O_5 with a balance of TiO_2, MgO and Na_2O, evaluated by averaging various sources from [3]. Park and Oh [10] reported an increase in viscosity with a larger amount of petcoke addition due to the formation of V_2O_3 crystal, which was assumed to cause difficulty of draining slags down the wall. V_2O_3 precipitates may also clog pores and microcracks of refractory liners lowering thermal shock resistance while it should impede the slag penetration into refractory. Kwong *et al.* found a solid solution containing Fe, V, Cr and Al at the interface between high chromia refractory and slag [7].

Although a description of the VO_x interaction with slag has not yet been optimized in the current databases of major thermodynamic software packages like FactSage [2, 11] or Thermo-Calc [16], the oxidation state of this transition metal can be predicted from the stability diagram as calculated in Figure 1 (Thermo-Calc ver.Q, TCFE2), under the assumption that molten slag does not kill the VO_x stability under the gasification conditions and that the formation kinetics is relatively fast. At 1500°C, vanadium oxide in air is thermodynamically stable as the liquid V_2O_5 phase, which, however, transforms to V_2O_3 if $\log(Po_2)$ = -8 (atm) is attained.

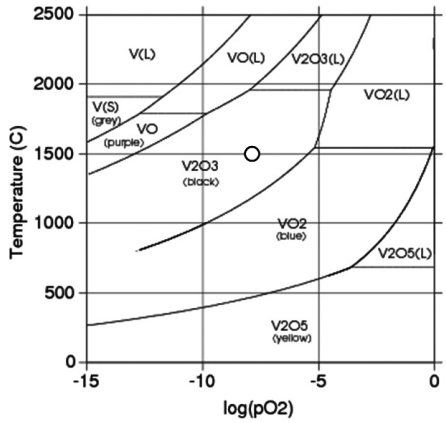

Figure 1: Stability diagram of VO_x over the partial pressure of oxygen (the present experimental condition is indicated by the empty circle)

This study focuses on the interfacial reactions between gasifier slags (coal and petcoke) and refractories (90wt.%Cr_2O_3-10wt.%Al_2O_3 and pure Al_2O_3) on a short-term and long-term basis, by utilizing Confocal Scanning Laser Microscopy (CSLM) to record *in situ* images of slag spreading behaviors on different refractory locations with different surface energies. Penetration of slags into different positions of these refractories was also studied from cross-sectioned samples, using Scanning Electron Microscopy (SEM) with X-ray Energy Dispersive Spectroscopy (EDS).

METHODOLOGY

Materials

The slags studied in this study were synthesized as follows (in wt.%): (i) coal slag (52SiO_2-24Al_2O_3-15Fe_2O_3-6CaO-3K_2O); and (ii) petcoke slag (25SiO_2-46V_2O_5-8Al_2O_3-10Fe_2O_3-10CaO-1K_2O). The coal ash slag composition was taken from a report of [15]. The chemistry of the petcoke slag was determined by averaging and normalizing data provided by [3] and the National Energy Technology Laboratory (NETL) in Albany. The slags were prepared by mixing appropriate amounts of oxide powders, which were heated above the melting temperature in Ar for two hours. The slags were premelted again under a CO/CO_2 (= 1.8) atmosphere at 1500°C for 20 minutes to minimize potential reducing reactions during the experiment. The CO/CO_2 (= 1.8) gas mixture provided an atmosphere of approximately log(Po_2) = -8 (atm) at 1500°C. The resultant compositions were tested by ICP (optical emission spectroscopy) and the results are shown in Table 1.

Table 1: Compositions of the slags used in this study (wt.%)

	Petcoke slag	Coal slag
SiO_2	25	52
Al_2O_3	7.8	24
CaO	10.1	6.4
Fe_2O_3	10.2	14.5
K_2O	1.2	2.9
V_2O_5	46	-
Total	100.3	99.8

Refractory samples used in this study were sinter-bonded high chromia-alumina (90 wt.%Cr_2O_3-10 wt.%Al_2O_3) and pure alumina (Al_2O_3). There are mainly two structurally distinct regions: grain aggregate parts where numerous grains are packed together (up to 3 mm in diameter); and powdery matrix regions where fine refractory particles are compacted with binding materials. The latter is more porous and is a weak link against chemical dissolution, mechanical erosion and slag penetration due to a large surface area and porosity network throughout the refractory. It should be noted that there are networking pores and microcracks across the grain aggregate as well. SEM micrographs of the refractory surfaces are shown in Figure 2.

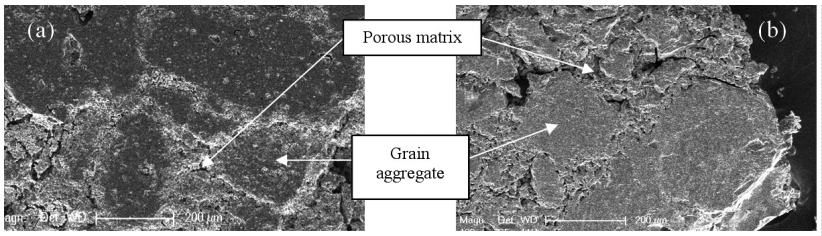

Figure 2: SEM images showing distinct microstructures of (a) alumina and (b) high chromia

High-Temperature Wetting Experiments

The interactions between the slag and the refractory were investigated by sessile drop type experiments and elemental mapping over different spatial locations with various grain/particle sizes. The degree of reactive wetting of the slags on each refractory material was recorded in-situ using a CSLM equipped with an IR-furnace. A sessile drop (300 to 500 µm) of each slag was placed separately on two different microstructures of a refractory plate (~ 1 mm thick, polished to 1 µm), and heated to 1500°C and held for 0 minutes and 10 minutes under a CO/CO_2 = 1.8 atmosphere. The average heating rate was 77°C/sec (100°C to 1500°C). After each heat treatment, the sample was gas-quenched with He, which achieved an average cooling rate of 99°C/sec (1500°C to 900°C). The reacted sample surfaces were analyzed with SEM-EDS. These samples were then cross-sectioned, vacuum mounted in epoxy and polished down to 1 µm for further analysis.

The cooling rate of 99°C/sec, which was much faster than the critical glass forming rate for slags [1], is assumed to minimize artifacts from slow cooling. However, it should be remembered that careful comparison of XRD patterns from quenched slag samples (cooling rate ~ 150°C/s) with real time high temperature XRD results, show that artifacts seem to be very difficult to completely eliminate [6].

A temperature gradient existed inside the heating chamber, which was created by a spatial deviation from the focal point as the heat source in a gold-coated ellipsoidal furnace. The deviation was estimated by utilizing pure Co whose melting point is known (= 1495ºC). By measuring apparent temperatures at which Co placed on the same experimental configuration started melting, a temperature calibration was carried out to determine the actual temperature of the slag sample on the refractory at the present experimental set-up. The average deviation was determined to be +55ºC. This gap was taken into account for all the experimental results.

In order to study the comprehensive nature of the slag-refractory interactions, the investigation was divided into 16 experiments: 2 slags (coal and petcoke) × 2 structurally different locations of refractory (grain aggregate and fined particles) × 2 refractories (90 wt.% Cr_2O_3-10wt.%Al_2O_3 and Al_2O_3) × 2 holding times (no soaking and 10 minutes). Note that the holding time here indicates a length of heat treatment after the designated temperature is reached. Therefore, potential reactions during heating must be also considered.

THERMODYNAMICS

Thermodynamically stable phases in terms of temperature and atmosphere can be predicted from computational aids. Phase fractions with respect to temperature were calculated using FactSage 5.5 with the FToxid Slag database (Figure 3). At the present experimental temperature (1500ºC), both slags are completely liquid and no solid is expected to form inside the slags at equilibrium. Crystalline phases, therefore, only form by interfacial reactions with the refractory materials, diffusion or supersaturation of the slag through dissolution of the refractory. Each homogeneity region is separated by thin dotted lines. For coal slag, there is a small amount of mullite ($2SiO_2{\cdot}3Al_2O_3$) coexisting with molten slag at 1300ºC, which decreases with higher temperatures. The slag becomes completely liquid above 1450ºC. In Figure 3(b), liquid petcoke slag is not predicted to be in equilibrium with any crystalline phase over the gasification temperature range (1300 – 1600ºC). Note that the computation for petcoke slag was done without VO_x and KO_x since no interaction data was available in FactSage and Thermo-Calc. However, according to Figure 1, V_2O_3 is likely to be stable with the molten slag in normal gasification conditions as the melting temperature of V_2O_3 is higher (>1890ºC [10]) than common gasification temperatures. The thermodynamic analysis of the V_2O_3 interaction with slag is underway.

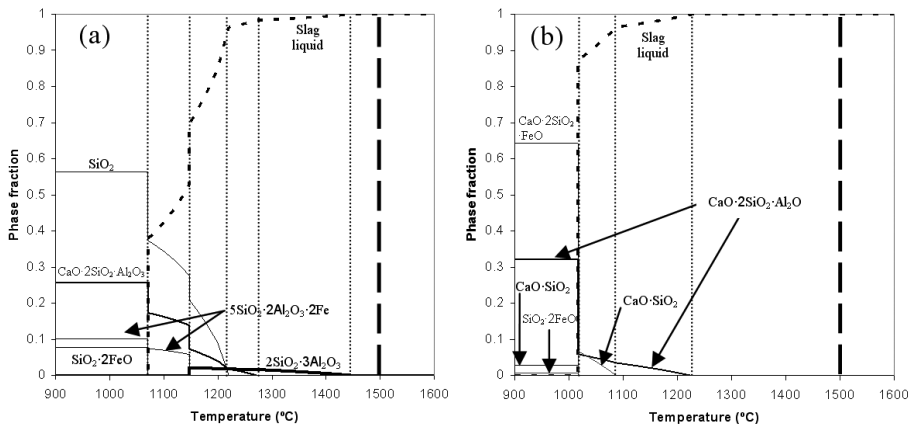

Figure 3: Phase fraction vs. temperature for (a) coal slag and (b) petcoke slag at log(Po_2) = -8 (atm) (dotted lines = phase homogeneity region, dashed line = the present experimental condition)

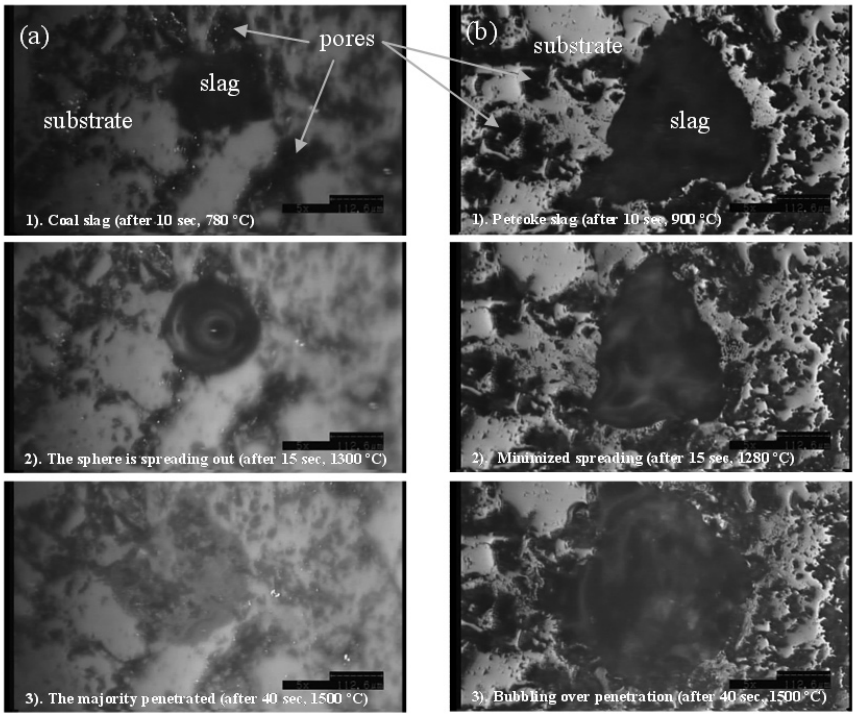

Figure 4: CSLM images showing wetting behaviors of (a) coal slag and (b) petcoke slag, over a fine grain matrix region of high chromia refractory

RESULTS

Surface images were taken from CSLM real time movies recorded during the heat treatments. A wetting mode of each slag type on a powdery region is compared in Figure 4. The majority of coal ash slag penetrated down the pores and microcracks of the refractory substrate 40 seconds after heating initiation. Petcoke slag started melting at lower temperatures and started rapidly spreading without forming a spherical shape. This wetting involved rapid bubbling as it drained into the refractory pores. Only small bubbles were observed with coal ash slag if placed on grain agglomerates. Note these bubbles were not caused by reduction reactions as no bubble was observed when the same slag was heated in a Pt-crucible under the same conditions. A spreading radius (relative to its original size) of petcoke slag was smaller than coal ash slag and the formation of VO_x- based solid phase was observed, which remained on the surface. If placed on grain agglomerates, a semispherical coal slag cap remained on the surface of both refractories after 10 minutes, whereas petcoke slag irregularly spread over the surface leaving VO_x- based particles.

SEM micrographs of the slags after reacting with different microstructures are shown in Figure 5 and Figure 6. Molten coal slag on a grain agglomerate remained on a surface in a semispherical form even after 10 minutes of heat treatments. Al_2O_3 particulates (10 – 30 μm) of the refractory were taken up into the coal slag and were washed out on the surface after the remaining liquid slag penetrated into the alumina substrate, whereas the coal slag almost completely penetrated during the interaction with the high chromia refractory. EDS elementary images of Cr and Si in Figure 7 represent high-Cr_2O_3 refractory substrate and coal slag, respectively. A pore network is strongly favored by the slag penetrating into the refractory.

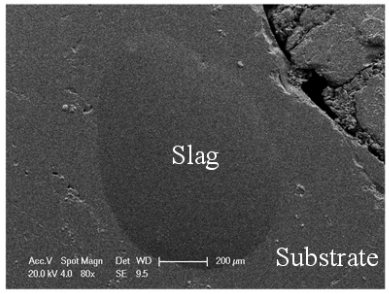

(a)
Coal slag on grain

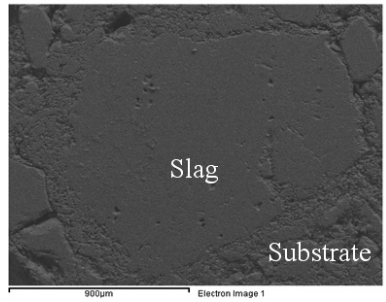

(c)
Petcoke slag on grain

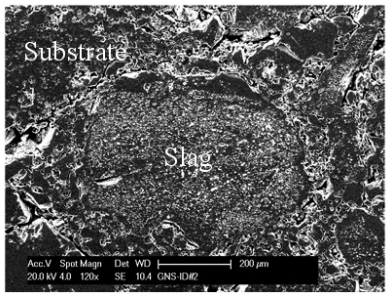

(b)
Coal slag on fined region

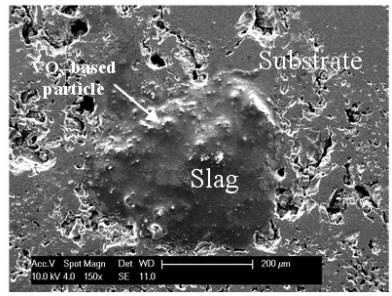

(b)
Petcoke slag on fined region

Figure 5: SEM micrographs of the slags on high chromia substrate after 10 minutes at 1500°C

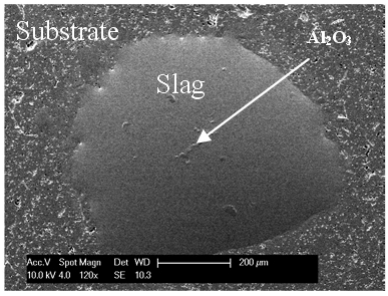

(a)
Coal slag on grain

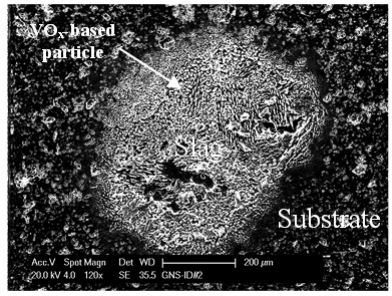

(c)
Petcoke slag on grain

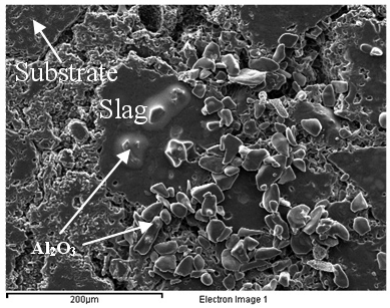

(b)
Coal slag on fined region

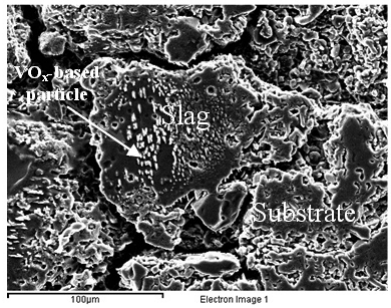

(b)
Petcoke slag on fined region

Figure 6: SEM micrographs of the slags on alumina substrate after 10 minutes at 1500°C

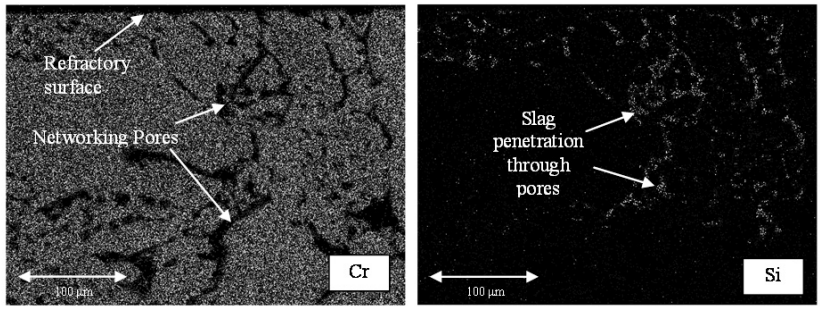

Figure 7: EDS maps showing coal slag (represented by Si on the right) favorably penetrating through pores of high chromia refractory (Cr)

DISCUSSION

The pertinent trends found in this study and remarks are briefly summarized:

- In comparison with coal slag, petcoke slag started initial deformation at lower temperatures and spread more rapidly involving vigorous bubbling. This was the case for both refractories.
- Wetting (or spreading) of the slags slowed down if placed on fined powdery portion of the refractory although more penetration was facilitated and slag species were detected at the bottom end of the refractories. A semispherical coal slag cap remained on a refractory surface during heat treatments, if placed on a grain aggregate. This was the case for both refractories.
- A crystallized phase (VO_x-based) formed inside the petcoke slag and at the slag/refractory interface. The majority of the VO_x phase was found above the surface for both microstructures and for both refractories. As a result, the slag that penetrated into the refractory was depleted in VO_x. Other elements were commonly found constituting the VO_x-based phase. The general tendency is: Cr-rich for high chromia refractory cases; and Fe-rich for alumina cases. The VO_x formation was also observed inside the refractory pores.
- In the case of the coal slag, a reaction phase was not noted with any of the refractories. Al_2O_3 agglomerates existed inside the slag, most likely due to particles being washed out from the refractory, and remained after saturation of the slag.

Critical Temperatures of Slags

The effects of the refractory materials and microstructures on the wetting behaviors of each slag can be further dictated by averaging the critical temperatures listed in Table 2. It must be noted that the local microstructures were identical in terms of variations in porosity and defects such as microcracks. Thus, while there is a significant difference between the grain agglomerate and the fine grained binder (Figure 2), there are also variations within each of these that were not quantified in this study.

As shown in Figure 5 and Figure 6, the slags reacted differently with different refractories. All of the critical temperatures of both slags tend to be higher for the Al_2O_3 refractory than the high chromia one. This phenomenon can be explained by two possible factors: (i) the melting temperature of the slag was raised by dissolving a larger quantity of Al_2O_3 into the slag than Cr_2O_3; and/or (ii) fast penetrating species escaped from the slag

amending the overall slag composition. There seems to be no apparent geometric effect of coal slag whereas higher critical temperatures were observed for petcoke slag, if the slag was placed on fine grain regions of high chromia. The opposite effect was found for alumina.

Wetting and Penetrating Behaviors of Slags

The spreading and penetrating behaviors are affected by: surface topology (including defects) and geometry (e.g. pores and micro-cracks); types of chemical reactions with the surface (formation of reaction layers and refractory dissolution); interfacial energy (e.g. grain agglomerates or fine powder); pore connectivity and networking; etc. The types of chemical reactions depend on the slag and refractory chemistry and process parameters.

Al_2O_3 grains from the Al_2O_3 refractory were taken up into the molten coal slag, which was commonly observed during CSLM recording. Figure 6 shows such Al_2O_3 grains that stayed in the molten coal slag after 10 minutes of heat treatment. Although mechanical removal can be induced by slag penetration attack, chemical dissolution has to be driven by the concentration jump at the interface, which was, however, minimized over time as the system approaches local equilibrium. Al_2O_3 grains can also be introduced into the slag when Al_2O_3 grains are regionally concentrated in the 90wt.%Cr_2O_3-10 wt.%Al_2O_3 refractory.

The Solid Formation (VO_x-Based)

By weight, close to half of the petcoke slag is comprised of vanadium oxide (VO_x). Vanadium is a transition metal which undergoes quite a few oxidation states corresponding to empirical conditions [4, 9, 13]. When the petcoke slag contacted the high chromia substrate, the fast VO_x-Cr_2O_3 interaction resulted in the immediate formation of the continuous (V, Cr, Fe)O_x crystal layer at the slag/refractory interface, impeding the slag penetration hereafter (Figure 8). The (V, Cr, Fe)O_x phase grew into the molten slag, which drifted away although the layer remained continuous during the 10 minute-soaking at 1500°C. The corresponding EDS maps indicated there was no noticeable amount of slag penetration through the layer. V was found at the bottom of the refractory in most of the cases, which implies some penetration of V-species occurred along with the slag liquid before the formation of VO_x. V-rich spherical particles were also found in the slag, which probably resulted from supersaturation with Cr_2O_3 and/or Al_2O_3 by refractory dissolution.

Table 2: A summary of experimental results (1500°C, log(Po_2) = -8 (atm))

Slag	Refractory	Structural location	Soaking (min)	IDTa (°C)	SFTb (°C)	SSTc (°C)	Predicted phase	Phase formed
Coal	High chromia	Grain	0	919	no	1304	None	-
Coal	High chromia	Grain	10	866	988	1139	None	-
Coal	High chromia	Matrix	0	932 625	1310 No	1329 877	None	-
Coal	High chromia	Matrix	10	977 873	1154 999	1236 1076	None	-
Coal	Alumina	Grain	0	1151	1406	1416	None	-
				1257	1325	1368		
Coal	Alumina	Grain	10	1146	1240	1408	None	$5SiO_2 \cdot 2Al_2O_3 \cdot 2FeO$
Coal	Alumina	Matrix	0	1177	1362	1382	None	-
Coal	Alumina	Matrix	10	1264 1045	1462 1168	1471 1247	None	-
Petcoke	High chromia	Grain	0	703	No	1051	V_2O_3	(V,Cr,Fe)O_x

Petcoke	High chromia	Grain	10	601	No	946	V_2O_3	$(V,Cr,Ca)O_x$
Petcoke	High chromia	Matrix	0	589	No	1166	V_2O_3	-
Petcoke	High chromia	Matrix	10	1067	No	1332	V_2O_3	$(V,Cr)O_x$
Petcoke	Alumina	Grain	0	1026	No	1457	V_2O_3	$(V,Fe)O_x$
Petcoke	Alumina	Grain	10	826	No	1276	V_2O_3	$(V,Si,Al)O_x$
Petcoke	Alumina	Matrix	0	861	No	1033	V_2O_3	$(V,Ca,Fe)O_x$
Petcoke	Alumina	Matrix	10	927	No	946	V_2O_3	VO_x-based

[a] Initial deformation temperature (measured when a pointing tip of slag started deforming)
[b] Sphere formation temperature (measured when slag liquid became spherical)
[c] Spread-starting temperature (measured when slag liquid started spreading)
[a,b,c] These temperatures are expected higher than the actual ones due to the fast heating rate.

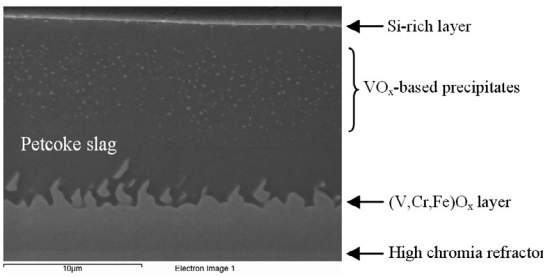

Figure 8: The formation of $(V, Cr,Fe)O_x$ at the petcoke slag/high chromia substrate interface

CONCLUSIONS

The wettability and penetration behavior of coal and petcoke slags on alumina and high chromia refractories were investigated. The petcoke slag showed a lower initial deformation temperature than the coal slag. The high chromia refractory, in general, exhibited a better corrosion/erosion resistivity against both slags with the exception that alumina outperformed when petcoke was placed on a fine grain portion of the refractories. A continuous layer of $(V, Cr, Fe)O_x$ instantly formed at the petcoke slag/high chromia substrate interface. Discrete particles of $(V, Al, Si)O_x$ also formed at the petcoke slag/alumina refractory interface.

ACKNOWLEDGEMENTS

This research was funded by the National Energy Technology Laboratory, U.S. Department of Energy, under contract NT41816. The authors thank Dr. Il Sohn (US Steel, Pittsburgh, PA) for carrying out ICP analyses for the synthetic slag compositions. Dr. Paolo Nolli (Vesuvius, Pittsburgh, PA) is also acknowledged for machining the refractory samples.

REFERENCES

Asayama, E., Takebe, H. & Morinaga, K. (1993). ISIJ International, 33(1), pp. 233-238. [1]

Bale, C. W., Chartrand, P., Degterov, S. A., Eriksson, G., Hack, K., Ben Mahfoud, R., Melançon, J., Pelton, A. D. & Petersen, S. (2002). CALPHAD, 26(2), pp. 189-228. [2]

Bryers, R. W. (1995). *Fuel Processing Technology.* 44, pp. 121-141. [3]

Johnston, W. D. (1965). J. American Ceramic Society, 48(12), pp. 608-611. [4]

Kashiwaya, Y., Cicutti, C., Cramb, A. & Ishii, K. (1998). ISIJ International, 38(4), pp. 348-356. [5]

Kashiwaya, Y., Cicutti, C., Cramb, A. & Ishii, K.(1998). ISIJ International, 38(4), pp. 357-365. [6]

Kwong, K., Petty, A., Bennett, J., Krabbe, R. & Thomas, H. (2007). *Applied Ceramic Technology.* 4(6), pp. 503-513. [7]

Lee, W. E. & Zhang, S. (1999). International Materials Reviews, 44(3), pp. 77-104. [8]

Mittelstädt, R. & Schwerdtfeger, K. (1990). Metallurgical Transsactions B, 21B, pp. 111-120. [9]

Park, W. & Oh, M. S. (2008). J. Industrial and Engineering Chemistry, 14, pp. 350-356. [10]

Pelton, A. D. (2006). Rare Metals, 25(5), pp. 473-480. [11]

Rewers, J., Kwong, J. & Bennett, J. (1999). *Materials at High Temperatures.* 16(4), pp. 219-222. [12]

Rovnushkin, V. A., Nikiforov, S. V. & Toporishchev, G. A. (1989). *Izvestiya Akademii Nauk SSSR*, Metally, 5, pp. 5-11. [13]

Schneider, H. & Komarneri, S. (2005). *Mullite.* Wiley-VCH, Weinheim, p. 325. [14]

Selvig, W. A. & Gibson, F. H. (1956). *Analyses of Ash from United States Coals.* Bureau of Mines Bulletin 567, United States Government Printing Office, Washington. [15]

Sundman, B., Janson, B. & Andesson, J.-O. (1985). CALPHAD, 9, pp. 153-190. [16]